

Predictive Coresets

Bernardo Flores
University of Texas at Austin

Abstract

Modern data analysis often involves massive datasets with hundreds of thousands of observations, making traditional inference algorithms computationally prohibitive. Coresets are selection methods designed to choose a smaller subset of observations while maintaining similar learning performance. Conventional coreset approaches determine these weights by minimizing the Kullback-Leibler (KL) divergence between the likelihood functions of the full and weighted datasets; as a result, this makes them ill-posed for nonparametric models, where the likelihood is often intractable. We propose an alternative variational method which employs randomized posteriors and finds weights to match the unknown posterior predictive distributions conditioned on the full and reduced datasets. Our approach provides a general algorithm based on predictive recursions suitable for nonparametric priors. We evaluate the performance of the proposed coreset construction on diverse problems, including random partitions and density estimation.

Keywords: coresets, predictive inference, Dirichlet process, optimal transport.

1 Introduction

We propose a construction of coresets based on a predictive view of Bayesian posterior inference (Fong et al., 2024; Fortini and Petrone, 2012). The main attraction of the approach is the model-agnostic nature - the method is valid with any inference model and independent of the specific inference goals, making it highly adaptable for a wide range of applications. Such adaptability is particularly valuable in the context of large-scale datasets, now commonplace in fields like genomics and astronomy. While this explosion of data offers incredible opportunities for discoveries, it also brings significant computational challenges. Tasks that were once straightforward, such as evaluating likelihoods several times have become increasingly difficult, making traditional data processing methods impractical. These obstacles have frequently pushed practitioners toward simpler statistical models that might not capture the full complexity of the data, disregarding expressiveness and flexibility that rich hierarchical and nonparametric models can offer.

Typically, scaling Bayesian inference for massive data involves tweaking specific algorithms like Markov Chain Monte Carlo (MCMC) or variational Bayes to handle data distributed across systems or streaming in real-time. Techniques such as mini-batches and streaming for variational Bayes (Hoffman et al., 2013) (Broderick et al., 2013a), subsampling methods for MCMC (Quiroz et al., 2018), and distributed methods for MCMC (Scott et al., 2016) are prominent examples. However, these existing methods have their drawbacks. In practice, subsampling MCMC methods often need to examine a significant portion of the data each time to be able to reach stationarity, which limits their efficiency gains (Johndrow et al., 2020). More scalable approaches like consensus MCMC and streaming variational Bayes improve computational efficiency but often lack rigorous theoretical backing and come with no guarantees for the quality of the proposed inference. A key observation in handling large datasets is that much of the data is redundant, while a smaller portion contains unique information. For instance, in a clustering setting, data points at the border of the cluster carry more discrimination power than the ones on the inside; moreover, adding two points close to each other does not add more structural information than just incorporating one of them. Similarly, in genome-wide association studies,

only a small proportion of genes actually are correlated to the target, which requires a careful control of the false discovery rate (Sesia et al., 2021).

Building upon these observations, a recent trend has been to focus on modifying the dataset itself rather than altering the inference algorithms. Specifically, to introduce a preprocessing step that constructs a coreset, a small, weighted subset of the original data that effectively approximates the inference with the full dataset. This coreset can be used with standard inference procedures to produce posterior approximations with guaranteed accuracy (Huggins et al., 2016). Coresets originated in computational geometry (Feldman, 2020). In the Bayesian context several algorithms have been developed with strong theoretical backings; see Campbell and Broderick (2019); Huggins et al. (2016); Manousakas et al. (2020); yet the nature of these approaches using likelihoods has limited the applications for deep hierarchical models and likelihood-free settings like non-Euclidean and simulator-based models (Winter et al., 2023).

In this paper we extend the concept of coresets by focusing on the posterior predictive distributions, rather than on the likelihoods; as well as using distances between probability measures instead of data points. This change of strategy allows us to include prior structure and to accommodate non-standard applications with data in non-Euclidean spaces.

In Section 2, we review existing coreset approaches. Section 3 introduces our novel coreset construction alongside a detailed algorithm. In Sections 4 and 5, we demonstrate the versatility of our method through three applications—parametric logistic regression, random partitions and density estimation. Section 6 establishes theoretical guarantees by analyzing posterior contraction rates. Finally, Section 7 outlines an extension of the algorithm from Section 3 that facilitates faster hyperparameter exploration, and we conclude with some final comments.

2 Coresets

Coresets are data summarizing methods designed to, given a data set and a learning algorithm, reduce the size of the dataset while retaining a similar learning performance (Campbell and Broderick, 2019). Typically one wishes to approximate a density π^N comprised of N potentials $\{f_n(\theta)\}_{n=1}^N$ and a base density π ,

$$\pi^N(\theta) = \frac{1}{Z} \exp\left(\sum_{n=1}^N f_n(y_n, \theta)\right) \pi(\theta).$$

In a Bayesian context, π is the prior distribution, f_n is the log-likelihood of the n th data point, and hence π^N is the posterior density. The approximation is formulated by defining a set of sparse weights $w = (w_n)_1^N$ such that only at most M weights are non-zero, where $M \ll N$, and then running the estimation algorithm on the weighted likelihood

$$p_\theta(w \odot y_{1:N}) = \frac{1}{Z(w)} \exp\left(\sum_{n=1}^N w_n f_n(y_n, \theta)\right),$$

where the operator \odot denotes the weighting by w . We denote the posteriors obtained under weights w as π_w^N . Whenever no weights are used—that is, when all weights are set to 1—we denote the coreset by π_1^N and refer to it as the unit coreset.

Finding the set of optimal weights w^* can be done in a variational way by minimizing the Kullback-Leibler (KL) divergence between the weighted posterior π_w^N and π_1^N , defined as

$$D_{KL}(\pi_w^N | \pi_1^N) = \int \pi_w^N \log \frac{\pi_w^N}{\pi_1^N}$$

Thus w^* is the solution of the optimization program

$$w^* := \arg \min_{w \in \mathbb{R}^N} D_{KL}(\pi_w^N | \pi_1^N) \quad \text{s.t.} \quad w \geq 0, \|w\|_0 \leq M,$$

where $\|w\|_0 := \sum_n \mathbb{1}(w_n > 0)$.

Many algorithms in this direction have been proposed; yet an open question remains; how to extend them to non-parametric settings. The difficulty arises from the fact that the normalizing constants are not available in a general functional form without integrating out some of the randomness and performing truncations.

Claici et al. (2020) proposed an alternative, variational view of coresets exploiting the machinery behind optimal transport theory (Villani, 2003). Recall that the p -Wasserstein distance between two probability measures μ and ν is defined as

$$W_p(\mu, \nu) = \inf_{\gamma \in \Pi(\mu, \nu)} \int \|x - y\|_p^{1/p} \gamma(dx, dy),$$

the infimum being taken over the set of couplings $\Pi(\mu, \nu)$ between μ and ν .

The idea is to introduce a variational family Π_θ and to find a measure $p_\theta \in \Pi_\theta$ that minimizes the p -Wasserstein distance with the likelihood p under the full data set, *i.e.*

$$\min_{p_\theta \in \Pi_\theta} W_p(p_\theta, p). \quad (1)$$

This was achieved by parametrizing the problem as finding a Lipschitz map T , so that given data y_1, \dots, y_N and a subsample of it y_1^*, \dots, y_n^* , T is obtained by solving

$$\min_T W_p \{ \hat{p}[T(y_{1:n}^*)], \hat{p}(y_{1:N}) \},$$

where \hat{p} denotes the empirical measure. Here and throughout we use notation y_i^* for the subsamples to highlight that the subsample is not restricted to the first n , but could be any subset of the full N data points. Note that (1) is equivalent to a Monge problem (Villani, 2003), heavily studied in optimal transport theory.

We leverage this approach on an analogous problem to develop a general methodology for constructing coresets for nonparametric models. Assume we observe data $y_1, \dots, y_N \sim p^0$ from an unknown model p^0 .

Following the principles of predictive inference (see Berti et al. (2023) for a review), uncertainty around p^0 can be thought of as being represented by missing data. If we had an infinite sample there would be no randomness left around p^0 . This suggests inference on the data-generating mechanism, no matter the method, is inherently done by learning the posterior predictive distribution.

To facilitate the presentation of our method, we summarize the notation used throughout the article in Table 1.

3 Predictive Coresets

We now provide a formal definition of predictive coresets. We use $p(x)$ denote the probability law of the random element x , and blackboard bold font like \mathbb{P} to denote random probability measures.

Definition 3.1. Given a sample $y_{1:N}$ and a subsample $y_{1:n}^*$, we define a **predictive coreset** as a measure $\tilde{\mathbb{P}}_n \propto \sum_{i=1}^n \delta_{\tilde{y}_i^*}$ given by the empirical distribution of $\tilde{y}_{1:n}^* = T(y_{1:n}^*)$, where T is the **coreset transform** determined by minimizing a discrepancy d between measures over a family of transformations \mathcal{T} :

$$T = \arg \min_{T \in \mathcal{T}} d [p(\tilde{y}_{n+1:\infty}^* | T(y_{1:n}^*)), p(\tilde{y}_{N+1:\infty} | y_{1:N})]. \quad (2)$$

The nature of $\tilde{\mathbb{P}}_n$ as a random probability measure arises from the random variables $\tilde{y}_{n+1:\infty}^*$ and $\tilde{y}_{N+1:\infty}$. Note that we use the additional tilde in $\tilde{y}_{n+1:\infty}^*$ to mark the implicit transform T .

The definition poses two methodological questions:

- (A) What is the most effective method to determine the conditional distributions in Equation (2)?
- (B) And how can we parameterize the family of transformations \mathcal{T} to ensure sufficient expressiveness?

Notation	Definition	Space
\cdot^N \cdot^*	Posterior distribution Related to a subsample	Any probability measure
π π_w	Prior distribution Weighted	Parameters Θ
p p_θ p_θ^w $p_N = p_{y_{1:N}}$ p^0 \tilde{y} F_θ	Likelihood Parametrized likelihood Likelihood based on weighted data Posterior predictive under a DP True distribution Samples of p_N Parametric family	Data \mathbb{X}
\hat{p} \mathbb{P}_θ	Empirical measure Law of p_θ or mixing measure	Probabilities $\mathcal{P}(\mathbb{X})$

Table 1: Table with notation for the probability measures used in throughout this work.

3.1 A proxy for the posterior predictives

The context of coreset approaches are problems where full posterior inference is not practically feasible. We therefore do not have access to the true posterior predictive distributions in (2), and need to approximate them in a way to ensure that the predictive coreset is consistent. For a generic description, suppose we aim to estimate a model F_θ for $\theta \in \Theta$. For example, F_θ could be the implied marginal distribution of the data under the inference model under consideration, including unknown hyperparameters θ .

We adopt the nonparametric learning (NPL) framework of Lyddon et al. (2018), which places a Dirichlet process (DP) prior (Ghosal and van der Vaart, 2017) centered at F_θ on the data-generating process p :

$$\begin{aligned}
y_1, \dots, y_N \mid \mathbb{P}_\theta &= p \sim p, \\
\mathbb{P}_\theta \mid \theta &\sim \text{DP}(F_\theta, \alpha), \\
\theta &\sim \pi(d\theta).
\end{aligned} \tag{3}$$

Here, $\pi(d\theta)$ is a hyperprior, which encodes any possible hierarchical structure in the model. The motivation for adopting (3) is that it will allow us a computation efficient approximation of the posterior predictive in (2). To start, the posterior distribution based on N data points under (3) is

$$p_\theta \mid y_{1:N} \sim \mathbb{P}_\theta^N = \text{DP}(F_\theta^N, \alpha + N),$$

where $F_\theta^N \propto \alpha F_\theta + N \hat{p}_N$, and $\hat{p}_N \propto \sum_{i=1}^N \delta_{y_i}$ is the empirical measure. The parameter α allows us to interpolate between the Bayesian bootstrap (Clyde and Lee, 2001) and sampling from F_θ . The idea here is that the posterior law under (3) is computationally easy. In particular, the DP provides a tractable approximation of the true posterior predictive under F_θ via the Pólya urn scheme, denoted p_N . Due to posterior consistency, the posterior predictives eventually concentrate around the true data-generating process p^0 . Explicit concentration rates will be provided in Section 6.

By considering two alternative ways to condition the DP, once conditioning on both the full data $y_{1:N}$ and once conditioning on the coreset support $y_{1:n}^*$, we can recursively sample trajectories $(y_{1:N}, \tilde{y})$ and $(y_{1:n}^*, \tilde{z})$. Here we use \tilde{y} and \tilde{z} , respectively, to denote the posterior predictive samples. We then compute the transformation T that minimizes the distance between these trajectories. An overall optimal mapping T is finally obtained via averaging Monte Carlo samples over these transformations. The complete procedure is detailed in Algorithm 1.

Recall the discrepancy $d(\cdot, \cdot)$ in (2). A key observation is the following: because we are adding uncertainty around the data-generating process, we must choose a discrepancy defined between random probability measures rather than fixed probability distributions. For a practical implementation (in the upcoming Algorithm 1) we switch the optimization and the prediction in (2). We carry out the optimization in (2) for each realization of an approximate posterior predictive draw for $\tilde{y}_{n+1:n+M}^*$ and $\tilde{y}_{N+1:N+M}$, and define T as the average of these optimizations. For a theoretical analysis we will use the Wasserstein metric with a Wasserstein base metric. Details of this definition are discussed later, in Section 7. This approach allows us to work with models over non-Euclidean spaces, such as partitions, by incorporating their topologies into the computation while requiring only well-behaved ground metrics.

3.2 Parametrization

Regarding the second question (B) about the target (2), by using the Wasserstein distance finding the optimal mapping becomes a Monge problem:

$$\inf_{T: T\#\mu=\nu} \int \|x - T(x)\| \mu(dx),$$

where the infimum is taken over all measurable maps T that push forward μ to ν . The goal is to find the transformation that minimizes the cost in the $\|\cdot\|$ norm. In the setting of (2), μ is the empirical over the augmented full data $\hat{p}[(y_{1:N}, \tilde{y}_{N+1:N+M})]$ and ν the empirical over the augmented coreset support $\hat{p}[(y_{1:n}^*, \tilde{y}_{n+1:n+M}^*)]$ and T is restricted to only transforming the actual observations $y_{1:N}$ and $y_{1:n}^*$.

Finding T is generally challenging. As highlighted by Hütter and Rigollet (2021), the computational complexity becomes prohibitive as the dimensionality increases, especially in nonparametric settings. Moreover, working with random measures requires Monte Carlo estimates of distances between samples of these measures, further amplifying the computational burden due to the need to compute the transport multiple times.

For simplicity, we opt for linear transport maps, that is, mappings of the form $T(y_1^*, \dots, y_n^*) = (w_1 y_1^*, \dots, w_n y_n^*)$; for brevity $y_{1:n}^* \mapsto w \odot y_{1:n}^*$. These have demonstrated good performance in various settings, offering sufficient flexibility to produce favorable results while possessing dimension-free contraction rates, thus avoiding the curse of dimensionality (Flamary et al., 2019). Further, because the M points sampled from the Pólya urn are not part of the coreset support, we restrict the weighting to only the observed data, leaving $y_{n+1:M+1}^*$ unmodified. Finally, we represent the posterior predictives by the empirical distribution of the M -step predictions.

With this we can give a full procedure, stated in Algorithm 1. To highlight the dependence of $\tilde{y}_{n+1:n+M}^*$ on the transformation T , i.e., ω , we write $\sigma(\omega, M) \equiv \tilde{y}_{n+1:n+M}^*$.

The algorithm formalizes the optimization of the distances between random probability measures in (2) by an average over minimizations using distances over approximate posterior predictive draws.

Recall questions (A) and (B) after Equation (2). We have addressed (A) by putting a DP prior on the data-generating distribution, which facilitates a simple way to obtain the posterior predictives. For (B), we chose to parametrize the family of transformations \mathcal{T} with affine maps over the observations, leaving the imputed predictions untouched. This way we obtained an efficient yet expressive algorithm sufficient for common applications. In the following section, we demonstrate the algorithm’s performance through several empirical examples.

4 Simulations

4.1 Density Estimation

We performed a simulation study with 100 repeat simulations. On each iteration we sampled $N = 1,000$ data points from a location mixture of three Gaussians with random parameters $\mu_j \sim N(0, \sigma^2)$, $j = 1, 2, 3$ and $\sigma^2 \sim \text{InvGamma}(1, 1)$.

We put an infinite mixture of Gaussians with a DP mixing measure prior on the density, and choose the 2-Wasserstein metric as discrepancy. The infinite mixture was fitted using Stein

Algorithm 1 Predictive coreset

- 1: Given a dataset $y_{1:N}$
- 2: Set a desired coreset size n
- 3: Sample coreset support $y_{1:n}^*$
- 4: **for** $t = 1, \dots, \text{niter}$ **do**
- 5: Sample $\theta_t \sim \pi(d\theta)$ from the priors.
- 6: Sample M points from the Pólya urn for the full data set implied by (3)

$$y_{N+1}, \dots, y_{N+M} \sim p_N$$

- 7: Let $\sigma(\omega, M) = \tilde{y}_{n+1:n+M}^*$ denote a size M sample from a weighted Pólya urn $p_{\omega \odot y_{1:n}^*}$ using weights $\omega = \omega_t$.
- 8: The weights ω_t are determined using (2), substituting the empirical distributions under approximate posterior predictive draws. That is,

$$\omega_t = \arg \min_{\omega} d[\hat{p}(y_{N+1:M}), \hat{p}(\sigma(\omega, M))],$$

where \hat{p} is the empirical distribution.

- 9: Return $\bar{\omega} = \frac{1}{\text{niter}} \sum w_t$
-

variational gradient descent (SVGD) (Liu and Wang, 2016) for the unit coreset, the predictive coreset and the full data, after which we recorded the discretized KL divergence between the posterior mean densities. To get the coreset we took a subsample of size $n = 50$ and sampled $M = 200$ times from the Pólya urn.

The results are shown in Figure 1a. The coreset improves the fit compared to the uniform subsample. Taking the data from one repeat simulation, we see that the weighting helps to recover the two separate modes compared to the unit weights, as for the former the estimated mean density was unimodal. Figure 1b shows a histogram of the difference in KL divergences $D_{KL}(\hat{f}_{\text{coreset}}, \hat{f}_{\text{full}}) - D_{KL}(\hat{f}_{\text{unit}}, \hat{f}_{\text{full}})$. In 81% of the repeat simulations the weighted coreset yielded a closer fit to the full data than the unit coreset, showing an overall good improvement.

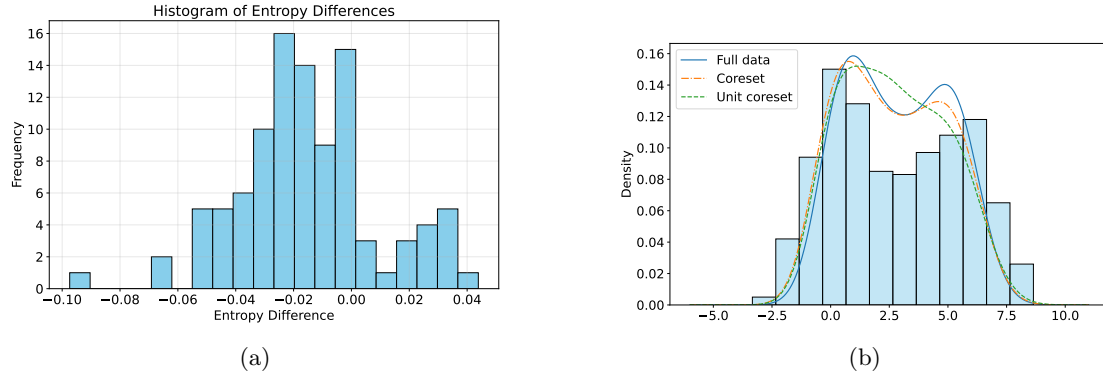


Figure 1: The left plot shows a histogram of the difference in estimated KL divergence between the posterior means for two cases: one comparing the coreset to the full dataset, and the other comparing the unit coreset to the full dataset. The right plot shows the posterior mean densities for all three cases.

4.2 Logistic Regression

Similarly to the first simulation, we performed 100 repetitions of the procedure described next:

We sampled 10,000 data points (x_i, y_i) , $i = 1, \dots, 10,000$ from a logistic regression by generating a continuous covariate and an intercept $x \sim N([0, 0], 5I)$ and using a vector of logistic regression coefficients $\beta \sim N([0.5, 0.5], I)$.

Note the sample space here is now $\mathcal{X} = \{0, 1\} \otimes \mathbb{R}^2$, as we cannot uncouple the response from the covariates. Thus we define a base metric on \mathcal{X} given by the product distance $d((x_1, y_1), (x_2, y_2))^2 = d_{L_2}(x_1, x_2)^2 + \mathbb{1}(y_1 \neq y_2)$, and as discrepancy we use d-Wasserstein distance.

To construct a coresets we need to now define a way of sampling from the empirical. The logistic regression gives a distribution for $y | x$, so to sample pairs (x, y) we need a distribution for x . We choose the empirical $x_1, \dots, x_n \sim F_n^x$, which corresponds to the usual bootstrap.

We then get a subsample of size 20, corresponding to 0.2% data. We sample 100 trajectories of size $M = 100$ of the predictive, and obtain the optimum weights using the 2d-Wasserstein distance with the ground metric d defined above.

After this we fitted a logistic regression with standard Gaussian priors on the coefficients using mean-field variational inference, obtained the posterior mean for the betas and registered the L_2 distance between the mean posterior logit functions based on the coresets and the unit coresets compared to the full data.

The results are shown in figure 2. We can see for one iteration the fitted logistic function with the predictive coresets is much closer to the one with the full data than the one with the unit coresets, *i.e.* with just subsampling. We also show a histogram with the L_2 differences between the mean posterior logit functions. We found 71% of the iterations yielded closer distances between the functions for the coresets than for the uniform subsample.

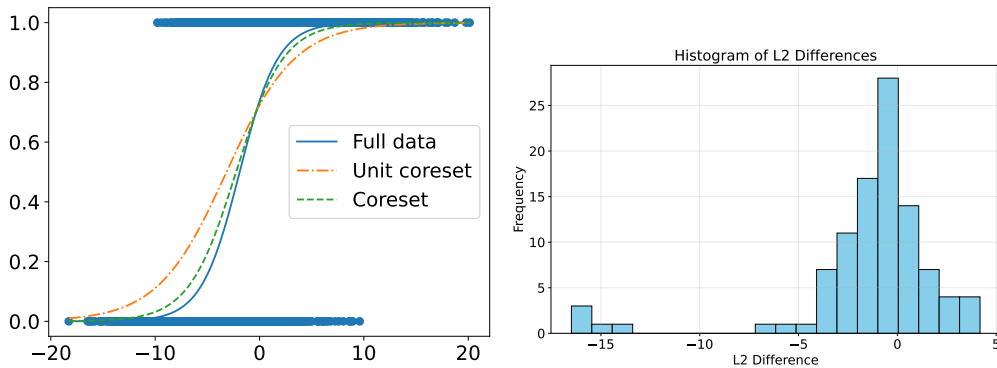


Figure 2: On the left is the results for a coresets of size 20; on the right the distance between the mean posterior logits for the coresets and the uniform subsample.

5 Coresets on random partitions

The predictive framework developed here facilitates the construction of coresets in non-Euclidean spaces. To illustrate this we consider coresets for random partitions. A key point to highlight is that, in many scenarios, we do not directly observe a random partition; instead, we observe data points y_i that we wish to cluster. This situation requires the notion of a mapping from the data space \mathcal{X} to the space of partitions of $[n] = \{1, \dots, n\}$. In a Bayesian context, inference on partitions is often based on mixture models, assuming that the data arise as

$$y_i | \theta_i \stackrel{\text{iid}}{\sim} k(\cdot | \theta_i), \quad \theta_i | \mathbb{P} \stackrel{\text{iid}}{\sim} \mathbb{P}, \quad \mathbb{P} \sim G. \quad (4)$$

where \mathbb{P} is a discrete random probability measure and $k(\cdot | \cdot)$ is a suitable kernel. Equation (4) is writing the mixture model $y_i \sim \int k(\cdot | \theta) d\mathbb{P}(\theta)$ as an equivalent hierarchical model. Interpreting latent indicators s_i that link the latent θ_i with the discrete point masses of \mathbb{P} as cluster membership indicators formalizes a random partition of experimental units $i = 1, \dots, n$. The construction is motivated by Kingman's representation theorem (Kingman, 1978) which shows that under certain symmetry conditions, including exchangeability, any random partition

can be thought of as arising this way. Let $\mathbf{s} = (s_1, \dots, s_n)$ denote the implied random partition (with or without ordering). For many choices of \mathbb{P} the implied probability function $p(\mathbf{s})$ can be conveniently represented in terms of an exchangeable partition probability function (EPPF) $f(\mathbf{n})$ where $\mathbf{n} = (n_1, \dots, n_K)$ are the cardinalities of the clusters under \mathbf{s} and $f(\mathbf{n})$ is a symmetric function of an additive decomposition (n_1, \dots, n_K) of n (Broderick et al., 2013b).

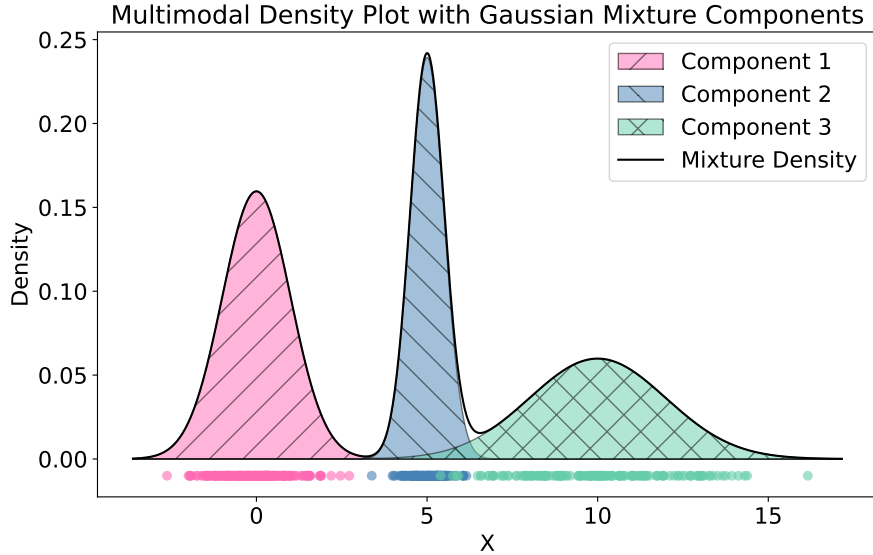


Figure 3: Data simulated from a mixture model, along with its induced clustering.

In summary, the posterior distribution resulting from (4) yields a sequence $\theta = (\theta_i)$, which can be mapped to a partition of $[n]$. A crucial distinction between this scenario and traditional density estimation is that density estimation operates directly within the space of densities supported over the observed data, whereas the earlier involves the pushforward of the posterior mixing measure into partitions. In essence, the data informs the posterior distribution \mathbb{P}^N , which then generates the predictive distribution mapping to an induced partition rather than back into the original data space. In short, the approach to define predictive coresets for a random partition in this context is to apply Algorithm 1, this time for the pairs (θ_i, y_i) .

Evaluating the effects of different coreset weights on the resulting partitions requires considering both the observed data (y_i) and the corresponding cluster indicators (s_i) , which are derived from the latent sequence (θ_i) . Since (θ_i) and (s_i) are latent variables, they must be imputed. A straightforward approach is to sample these variables from $p(\mathbf{s})$ and $p(\theta | \mathbf{s})$, respectively, thereby generating a new allocation vector \mathbf{s} and corresponding latent θ_i values at each iteration. This procedure then enables us to compute the posterior predictive distribution by calculating the Wasserstein distance between the empirical distributions of the mixing measures.

First, the parameters (θ_i) are sampled for the coreset support (y_i) from the implied marginal prior under (4); from them the cluster assignments (s_i) are obtained, after which the data is augmented as (y_i, s_i) . At this stage, depending on the model, there are two possible paths to follow. If the distribution on partitions allows for a closed-form posterior predictive distribution, one can directly sample the cluster assignments s_{N+j} from $p(s_{N+1:M} | y_{1:N})$ and then generate the data \tilde{y}_{N+j} conditioned on these assignments and a cluster-specific distribution G_{θ_i} . To obtain an approximate posterior for G_{θ_i} we assume a Dirichlet process prior with base measure $k(\cdot | \theta_i)$ and concentration parameter α .

If the distribution on $s_{N+1:M}$ cannot be updated in a closed form, the approach differs. In this case, the Dirichlet process base measure in (3) can be extended as $k(dy_i | \theta_i) \otimes \rho(d\theta_i)$. Here, cluster assignments are sampled implicitly by sampling θ_i using the Pólya urn for the pairs (y_i, θ_i) , a method that contrasts with the direct posterior updates used in the former scenario. The full procedure is shown in Algorithm 2. Note that, in general, we do not need to compute distances between the cluster assignments s_k but between the θ_k .

Algorithm 2 Predictive coresets for partitions (conjugate update)

- 1: Given a dataset $y_{1:N}$
- 2: Set desired coreset size n
- 3: Sample a subset $y_{1:n}^*$
- 4: **for** $t = 1, \dots, \text{niter}$ **do**
- 5: Sample clustering for the full data from the prior under (4),

$$\theta_{1:N} \sim p(\boldsymbol{\theta} \mid \mathbf{s}, y_{1:N}).$$

- 6: Extract $\theta_{1:n}^*$ and the implied partition $s_{1:n}^*$ from $\theta_{1:N}$.
- 7: Sample $\{(y_{N+j}, \theta_{N+j}); j = 1, \dots, M\}$ from the Polya urn for $\{(\theta_i, y_i); i = 1, \dots, N\}$.
- 8: Get

$$\omega_t = \arg \min_{\omega} d(\widehat{p}(y_{N+1:M}), \widehat{p}(\sigma(\omega, M))),$$

where σ is now extended to include the θ_k^* .

- 9: Return $\bar{\omega} = \frac{1}{M} \sum \omega_t$.
-

Algorithm 2 is simply implementing Algorithm 1 for the pairs (y_i, θ_i) , including only the one additional step of generating the random partition in step 5. And posterior predictive sampling in step 8 is extended to include θ_i^* .

Analogously to the previous simulation studies, we repeated the following 100 times: we sampled $N = 10,000$ observations from a Gaussian mixture with 6 components and recorded cluster memberships. We then sampled 50 observations uniformly and obtained the coreset weights with $M = 500$ posterior predictive simulations and the L_2 distance on the θ_i . A DP mixture of Gaussians was then fit using Stein gradient variational inference with an ordering constraint on the means to avoid label switching.

To obtain a point estimate for clustering we took the mode of the cluster assignments across 100 posterior simulations. The results are shown in Figures 4 and 5. The first figure shows the approximate posterior inference for a randomly chosen repeat simulation, whereas the second one shows a histogram with the difference in variation of information Meilä (2007) between the coreset and the full data, and the subsample and the full data. We found the coreset yielded a closer inference to the one based on full data than just the subsample in 91% of the samples.

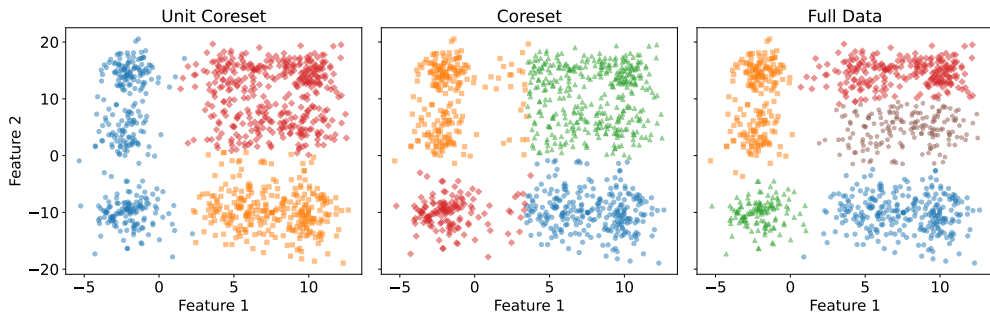


Figure 4: The panels show approximate posterior inference using a uniformly chosen core set (left), the proposed core set using Algorithm 3 (center) and full posterior inference (right).

6 Theoretical analysis

We give properties of the predictive coresets that guarantee their asymptotic performance. Moreover, we discuss how non-asymptotic consistency results can inform the selection of an appropriate coreset size. Specifically, given a base metric space (\mathcal{X}, d) , we equip the space of distributions

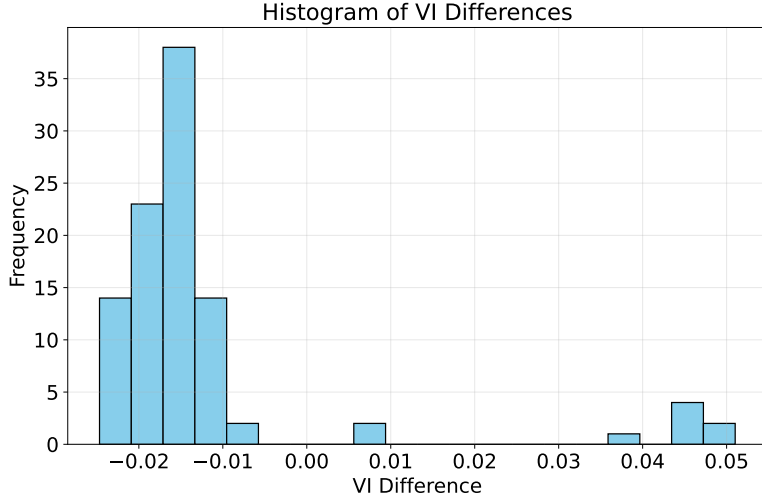


Figure 5: Histogram of the differences in variation of information between the coreset and the full data, and the subsample and the full data.

$\mathbb{P}(\mathbb{X})$ with the Wasserstein metric W_d , and then consider $(\mathcal{P}(\mathcal{P}(\mathbb{X})), W_{W_d})$. For simplicity, we denote $\mathfrak{d} = W_{W_d}$ and $d = W_d$.

Algorithm 1 computes a functional of two posterior predictive distributions, which themselves are functions of a random measure: the posterior distribution. Thus to provide contraction rates we will work with the Wasserstein over Wasserstein topology (emphc.f Catalano and Lavenant (2024)). This corresponds to endowing $\mathcal{P}(\mathcal{P}(\mathbb{X}))$, the space of random probability measures over \mathbb{X} with the Wasserstein distance with ground metric again the p -Wasserstein distance over \mathbb{X} .

The strategy now is to first obtain a posterior contraction rate, use it to get convergence and to establish a rate of convergence for the posterior predictives and then use a Cauchy sequence argument combined with optimal transport theory to get a rate of how close the weighted data set obtained from Algorithm 1 can get to the inference with the full data.

First we restate the main result from Camerlenghi et al. (2022) for the DP.

Theorem 1. *Assume that $(\mathbb{X}, \mathfrak{d})$ is a totally bounded metric space with packing number of order $N_\delta(\mathbb{X}, \mathfrak{d}) \sim \frac{1}{\delta^a}$ for some $a > 0$ and small enough $\delta > 0$. Then the following is a posterior contraction rate for the Dirichlet process with mean measure H , precision α and truth p^0 in the q -Wasserstein metric:*

$$\epsilon_n = \epsilon_{n,q}(\mathbb{X}, p^0) + n^{-(a+q)/2},$$

with $\epsilon_{n,q}(\mathbb{X}, p^0)$ being the q -Wasserstein rate of convergence of the Glivenko-Cantelli theorem for H , giving a q -Wasserstein posterior contraction rate at p^0 .

The $\epsilon_{n,q}$ term is of order $o_P \left(Y(p^0) [\log \log n/n]^{1/2q} \right)$ assuming p^0 has enough finite moments and r -dimensional Euclidean support. Notably, this rate is independent of the total mass α . The quantity $Y(p^0)$ has a complex form depending on the dimension r and the $2q + \delta$ moment of p^0 for some $\delta > 0$, see Dolera and Regazzini (2019) for more details.

For example, when p^0 a multivariate Gaussian with mean m_0 and covariance matrix V_0 it takes the form $Y(m_0, V_0) = \sqrt{2} \left\{ \sigma_{\max}[V_0] + d\sqrt{K(\varepsilon, r)\text{tr}(V_0)} \right\}$ for small enough $\varepsilon > 0$, where σ_{\max}^2 stands for the largest eigenvalue and $K(\varepsilon, r)$ is a positive constant. We can use this to show that Algorithm 1 converges.

Theorem 2. *As the number of simulations grows $n_t \rightarrow \infty$ the weights converge a.s.*

$$\lim_{n_t \rightarrow \infty} \frac{1}{n_t} \sum_{k=1}^{n_t} w_k = \arg \min_{\omega} d(p(\cdot | \omega \odot y_{1:n}), p(\cdot | y_{1:N}))$$

Proof. This is a consequence of the consistency of the posterior predictive for the DP given by the Glivenko-Cantelli theorem (Camerlenghi et al., 2022), as when $n_t \rightarrow \infty$, both distributions converge in the Wasserstein space to the true data generating distribution p_0 , provided the weighting map $\varpi_w : \sum \delta_{x_i} \mapsto \sum \delta_{w_i x_i}$ is continuous.

The map $w_i \mapsto w_i \odot x_i$ is continuous in any Banach space (\mathbb{X}, d) . Take $\varepsilon > 0$ and a discrete measure $\nu \in \mathcal{P}(\mathbb{X})$ with atoms $x = (x_i)$. Considering the independent coupling between $\varpi_{w_1} \nu$ and $\varpi_{w_2} \nu$ we get from a change of variables, take $\delta > 0$ and two vectors of weights w_1, w_2 such that $\|w_1 - w_2\|_2 < \delta$ implies $d(w_1 \odot x, w_2 \odot x) < \varepsilon$, which always exists by continuity. Now

$$\begin{aligned} W_d(\varpi_{w_1} \nu, \varpi_{w_2} \nu) &\leq \int d(y, z) d\varpi_{w_1} \nu d\varpi_{w_2} \nu \\ &= \int d(w_1 y, w_2 z) \nu(dy) \nu(dz) \\ &\leq \varepsilon, \end{aligned}$$

Thus the map ϖ_w is continuous. □

We can now give a first bound.

Theorem 3. *The posterior predictives satisfy for any $M_n \rightarrow \infty$*

$$d(\mathbb{P}_N, \mathbb{P}_n) = o_P(M_n \epsilon_{N,n}),$$

where $\epsilon_{N,n} = \epsilon_N + \epsilon_n$.

Proof. The posterior predictive of the DP is given by the generalized Pólya urn, whose one-step transition is the mean posterior measure (Ghosal and van der Vaart, 2017). Nguyen (2016) showed the DP is isometric to its mean measure in any q -Wasserstein space. So by definition of posterior contraction rates for every sequence $M_n \rightarrow \infty$

$$\begin{aligned} P(d(\mathbb{P}_n, p_0) > M_n \epsilon_n \mid x_1, \dots, x_n) &= P(d(\mathbb{P}_n^\theta, \delta_{p_0}) > M_n \epsilon_n \mid x_1, \dots, x_n) \\ &\longrightarrow 0 \quad p_0 - \text{ a.s.} \end{aligned}$$

Now, using the triangle inequality

$$d(\mathbb{P}_N, \mathbb{P}_n) \leq d(\mathbb{P}_N, p_0) + d(\mathbb{P}_n, p_0),$$

thus

$$P(d(\mathbb{P}_n, \mathbb{P}_N) \leq M_n (\epsilon_n + \epsilon_N) \mid x_1, \dots, x_n) \longrightarrow 1 \quad p_0 - \text{ a.s.}$$

This implies that p_0 almost surely $d(\mathbb{P}_n, \mathbb{P}_N) = o_P(M_n (\epsilon_n + \epsilon_N))$. □

This gives a (loose) upper bound of the error we are trying to minimize. We can interpret the rate by looking at the $\epsilon_{N,n}$ term. First note that this gives a family of rates so that as n grows the distance between both distributions diminishes; moreover, the fact this bound was derived from a posterior contraction rate gives a non-asymptotic result on the shape of the Wasserstein balls so that with high probability the posterior predictive based on the sub-sample is at most at $\epsilon_{N,n}$ from the one based on the full data.

Finally we will discuss the implications of the coresets weights, namely how much can it improve over $\epsilon_{N,n}$. This can be translated to the expressiveness of the coresets transform, as if $w \odot \mathbb{P}_n$ can match \mathbb{P}_n , then the σ -algebras generated by both point clouds would be identical.

Foremost, the transformation $T_w : \mu \mapsto w \odot \mu$ can be interpreted as a transport plan between \mathbb{P}_n and \mathbb{P}_N . Affine Monge maps have been shown to be reasonably well behaved for Euclidian settings in the W_2 space Flamary et al. (2019), achieving good generalization bounds while retaining computational efficacy. Our intercept-free setting retains the same properties by centering the samples.

7 An adaptive extension and conclusion

Among the limitations of the proposed approach is in particular the prior simulation (in Step 5 of Algorithm 1), which can lead to very inefficient approximations of the posterior predictive used for equation (2). Before we conclude with a broader discussion of limitations and extensions, we briefly outline a possible strategy to mitigate this limitation.

We introduce an extension of the basic predictive coreset algorithm aimed at reducing its computational burden, particularly in hierarchical models with multiple layers of hyperparameters. In the standard versions of Algorithms 1 and 2, the predictive trajectories are generated by independent sampling from the hyperpriors (in Step 5 of Algorithm 1) sampling uniformly from the hyperpriors. However, in high-dimensional or deep hierarchical settings, this approach can be exceedingly slow because many sampled hyperparameter values lie in regions of negligible posterior mass, leading to a large fraction of wasted trajectories.

To address this issue, we draw inspiration from Wasserstein Approximate Bayesian Computation (Wasserstein-ABC) methods (Bernton et al., 2019). The idea is to replace uniform sampling over the priors with an MCMC-based sampling scheme, focusing exploration on regions of the hyperparameter space Θ with high (approximate) posterior probability. This selective sampling strategy reduces computational overhead by concentrating on the portions of the parameter space that are most relevant for the model’s predictive performance.

Our proposed algorithm employs a Metropolis-Hastings (MH) kernel. Specifically, after drawing a candidate hyperparameter θ^* from a proposal distribution $\pi(d\theta^* | \theta_{t-1})$, we accept θ^* with a probability derived from an approximation to the usual likelihood ratio. Let $p_\theta(dz)$ denote the sampling model. Recall that that in ABC, one aims to approximate the (unknown) posterior

$$p^\varepsilon(d\theta | y_{1:N}) \propto \pi(d\theta) \int \mathbb{1}(d(y_{1:n}, z_{1:n}) \leq \varepsilon) p_\theta(dz_{1:n}),$$

where z is hypothetical data generated from $p_\theta(dz)$ and $d(\cdot, \cdot)$ is a user-chosen discrepancy function, and $\varepsilon > 0$ is the ABC tolerance parameter. Because we generally do not have direct access to the likelihood p_θ , we construct a Monte Carlo approximation by simulating data from p_θ repeatedly, yielding

$$\hat{p}^\varepsilon(d\theta | y_{1:N}) \propto \pi(d\theta) \sum_t \mathbb{1}(d(y_{1:n}, z_{1:n}^t) \leq \varepsilon),$$

where $z_{1:n}^t$ is the t -th simulated dataset of size n from the model p_θ . Denoting $z_{\theta, 1:n}^t$ a sample of size n from p_θ and assuming a symmetric proposal distribution, the acceptance probability in the Metropolis-Hastings step becomes

$$\rho(\theta^* | \theta) = 1 \wedge \frac{\pi(d\theta^*) \sum_t \mathbb{1}(d(y_{1:n}, z_{\theta^*, 1:n}^t) \leq \varepsilon)}{\pi(d\theta) \sum_t \mathbb{1}(d(y_{1:n}, z_{\theta, 1:n}^t) \leq \varepsilon)}.$$

This ratio reflects how likely the newly proposed hyperparameter θ^* is to generate simulated data close (under d) to the observed data $y_{1:n}$, compared with the current hyperparameter θ . Once accepted, θ^* typically leads to predictive trajectories that are more likely to arise from a region of Θ with higher approximate posterior mass.

7.1 Overview of the adaptive algorithm

Algorithm 3 describes the complete adaptive process. At each iteration, a candidate hyperparameter θ^* is generated from a proposal distribution centered at the current state θ_{t-1} . Next, several pseudo-datasets $z_{\theta^*, 1:n}^t$ are simulated from p_{θ^*} . Using these simulations, the acceptance ratio $\rho(\theta^* | \theta)$ is computed based on the ABC posterior approximation. Finally, θ^* is either accepted or rejected according to $\rho(\theta^* | \theta)$, with the accepted state becoming θ_t .

By iterating this procedure, we sample hyperparameters with a frequency proportional to their approximate posterior weight, thereby reducing the generation of wasted trajectories that are unlikely to contribute meaningfully to the model’s predictive accuracy. The full adaptive algorithm is given in Algorithm 3.

Algorithm 3 Adaptive predictive coreset

- 1: Given a dataset $y_{1:N}$
- 2: Set desired coreset size n
- 3: Sample coreset support $y_{1:n}^*$
- 4: **for** $t = 1, \dots, \text{niter}$ **do**
- 5: Sample a proposal $\theta^* \sim \pi(\theta)$ from the hyperpriors.
- 6: Accept $\theta_t = \theta^*$ with probability $\rho(\theta^*|\theta)$, otherwise set $\theta_t = \theta_{t-1}$.
- 7: Sample M points from the Pólya urn for the full data set

$$y_{N+1}, \dots, y_{N+M} \sim p_N$$

- 8: Let $\sigma(\omega, M) = \tilde{y}_{n+1:n+M}^*$ denote a size M sample from a weighted Pólya urn $p_{\omega \odot y_{1:n}^*}$ using weights ω .
- 9: The weights are determined using (2), substituting the empirical distributions under approximate posterior predictive draws. That is,

$$\omega_t = \arg \min_{\omega} d(\hat{p}(y_{N+1:M}), \hat{p}(\sigma(\omega, M))),$$

where \hat{p} is the empirical distribution.

- 10: Return $\bar{\omega} = \frac{1}{M} \sum \omega_t$
-

7.2 Discussion

In this work, we proposed a novel construction of coresets for Bayesian inference by approximating predictive distributions rather than directly matching posteriors. This approach is both model-agnostic and scalable, making it particularly well-suited for large-scale datasets. Building on recent advances in computational optimal transport and Bayesian nonparametrics, we developed a simple yet flexible algorithm that performs well across diverse settings, including nonparametric scenarios that were previously out of reach for traditional coreset construction methods.

Despite its flexibility and strong empirical performance, the proposed approach has certain limitations. While we emphasize its model-agnostic nature, the method is not entirely free from modeling assumptions. Specifically, the approximation of the posterior predictive with a DP relies on exchangeability, which may not hold in all practical scenarios. Additionally, the prior sampling for hyperparameters can be computationally inefficient, particularly when dealing with high-dimensional parameter spaces, potentially limiting scalability in such cases. Another important consideration is the choice of the transformation T , which plays a crucial role in the coreset construction. Poor parametrization of T can significantly affect the performance and robustness of the algorithm, highlighting the need for principled strategies for selecting or learning T in future work.

Acknowledgements

I am grateful to my advisor, Peter Müller, for his guidance, valuable discussions, and constructive feedback throughout this research.

Supplementary Material

Code: all code used to generate the results presented in this paper is publicly available at github.com/BernardoFL/Predictive-coresets.

References

- E. Bernton, P. E. Jacob, M. Gerber, and C. P. Robert. Approximate Bayesian computation with the Wasserstein distance. *Journal of the Royal Statistical Society Series B: Statistical Methodology*, 81(2):235–269, 02 2019.
- P. Berti, E. Dreassi, F. Leisen, L. Pratelli, and P. Rigo. Bayesian predictive inference without a prior. *Statistica Sinica*, 33:2405–2429, 2023. doi: 10.5705/ss.202021.0238.
- T. Broderick, N. Boyd, A. Wibisono, A. C. Wilson, and M. I. Jordan. Streaming variational Bayes. In C. Burges, L. Bottou, M. Welling, Z. Ghahramani, and K. Weinberger, editors, *Advances in Neural Information Processing Systems*, volume 26. Curran Associates, Inc., 2013a.
- T. Broderick, J. Pitman, and M. I. Jordan. Feature allocations, probability functions, and paintboxes. *Bayesian Analysis*, 8:801–836, 2013b.
- F. Camerlenghi, E. Dolera, S. Favaro, and E. Mainini. Wasserstein posterior contraction rates in non-dominated Bayesian nonparametric models. 2022. URL [arxiv:2201.12225](https://arxiv.org/abs/2201.12225).
- T. Campbell and T. Broderick. Automated Scalable Bayesian Inference via Hilbert Coresets. *Journal of Machine Learning Research*, 20(15):1–38, 2019.
- M. Catalano and H. Lavenant. Hierarchical integral probability metrics: A distance on random probability measures with low sample complexity. In R. Salakhutdinov, Z. Kolter, K. Heller, A. Weller, N. Oliver, J. Scarlett, and F. Berkenkamp, editors, *Proceedings of the 41st International Conference on Machine Learning*, volume 235 of *Proceedings of Machine Learning Research*, pages 5841–5861. PMLR, 07 2024.
- S. Claiici, A. Genevay, and J. Solomon. Wasserstein Measure Coresets. 03 2020. URL [arxiv:1805.07412](https://arxiv.org/abs/1805.07412).
- M. Clyde and H. Lee. Bagging and the Bayesian bootstrap. In T. S. Richardson and T. S. Jaakkola, editors, *Proceedings of the Eighth International Workshop on Artificial Intelligence and Statistics*, volume R3 of *Proceedings of Machine Learning Research*, pages 57–62. PMLR, 01 2001.
- E. Dolera and E. Regazzini. Uniform rates of the Glivenko–Cantelli convergence and their use in approximating Bayesian inferences. *Bernoulli*, 25(4A):2982–3015, 11 2019.
- D. Feldman. Core-sets: An updated survey. *WIREs Data Mining and Knowledge Discovery*, 10(1):e1335, 2020.
- R. Flamary, K. Lounici, and A. Ferrari. Concentration bounds for linear Monge mapping estimation and optimal transport domain adaptation. 2019. URL [arxiv:1905.10155](https://arxiv.org/abs/1905.10155).
- E. Fong, C. Holmes, and S. G. Walker. Martingale posterior distributions. *Journal of the Royal Statistical Society Series B: Statistical Methodology*, 85(5):1357–1391, 02 2024.
- S. Fortini and S. Petrone. Predictive construction of priors in Bayesian nonparametrics. *Brazilian Journal of Probability and Statistics*, 26(4):423 – 449, 2012.
- S. Ghosal and A. van der Vaart. *Fundamentals of Nonparametric Bayesian Inference*. Cambridge Series in Statistical and Probabilistic Mathematics. Cambridge University Press, 2017.
- M. D. Hoffman, D. M. Blei, C. Wang, and J. Paisley. Stochastic variational inference. *Journal of Machine Learning Research*, 14(1):1303–1347, 05 2013.
- J. H. Huggins, T. Campbell, and T. Broderick. Coresets for scalable Bayesian logistic regression. In *Proceedings of the 30th International Conference on Neural Information Processing Systems, NIPS’16*, page 4087–4095. Curran Associates Inc., 2016.
- J.-C. Hütter and P. Rigollet. Minimax estimation of smooth optimal transport maps. *The Annals of Statistics*, 49(2):1166 – 1194, 2021. doi: 10.1214/20-AOS1997.

- J. Johndrow, N. Pillai, and A. Smith. No free lunch for approximate mcmc. 10 2020. URL [arxiv:2010.12514](https://arxiv.org/abs/2010.12514).
- J. F. C. Kingman. Uses of exchangeability. *The Annals of Probability*, 6(2):183–197, 1978.
- Q. Liu and D. Wang. Stein variational gradient descent: A general purpose Bayesian inference algorithm. In D. Lee, M. Sugiyama, U. Luxburg, I. Guyon, and R. Garnett, editors, *Advances in Neural Information Processing Systems*, volume 29. Curran Associates, Inc., 2016.
- S. Lyddon, S. Walker, and C. C. Holmes. Nonparametric learning from Bayesian models with randomized objective functions. In *Advances in Neural Information Processing Systems*, volume 31. Curran Associates, Inc., 2018.
- D. Manousakas, Z. Xu, C. Mascolo, and T. Campbell. Bayesian pseudocoresets. In H. Larochelle, M. Ranzato, R. Hadsell, M. Balcan, and H. Lin, editors, *Advances in Neural Information Processing Systems*, volume 33, pages 14950–14960. Curran Associates, Inc., 2020.
- M. Meilă. Comparing clusterings—an information based distance. *Journal of Multivariate Analysis*, 98(5):873–895, 2007.
- X. Nguyen. Borrowing strength in hierarchical Bayes: Posterior concentration of the Dirichlet base measure. *Bernoulli*, 22(3):1535–1571, 2016.
- M. Quiroz, M. Villani, R. Kohn, and M.-N. Tran. Subsampling MCMC – an introduction for the survey statistician. *Sankhya A*, 80(Suppl 1):33–69, 2018.
- S. L. Scott, A. W. Blocker, and F. V. et al. Bayes and big data: the consensus Monte Carlo algorithm. *International Journal of Management Science and Engineering Management*, 11(2):78–88, 2016.
- M. Sesia, S. Bates, E. Candès, J. Marchini, and C. Sabatti. False discovery rate control in genome-wide association studies with population structure. *Proceedings of the National Academy of Sciences*, 118(40), 2021.
- C. Villani. *Topics in Optimal Transportation*. Graduate studies in mathematics. American Mathematical Society, 2003.
- S. Winter, T. Campbell, L. Lin, S. Srivastava, and D. B. Dunson. Machine learning and the future of Bayesian computation, 2023. URL [arxiv:2304.11251](https://arxiv.org/abs/2304.11251).